Inorganic Chemistry

Article

pubs.acs.org/IC

Structural Basis for Bifunctional Zinc(II) Macrocyclic Complex Recognition of Thymine Bulges in DNA

Imee Marie A. del Mundo,[†] Kevin E. Siters,[†] Matthew A. Fountain,*[,‡] and Janet R. Morrow*[,†]

[†]Department of Chemistry, University at Buffalo, State University of New York, Buffalo, New York 14260, United States

[‡]Department of Chemistry and Biochemistry, State University of New York, College at Fredonia, Fredonia, New York 14063, United States

Supporting Information

ABSTRACT: The zinc(II) complex of 1-(4-quinoylyl)methyl-1,4,7,10-tetraazacyclododecane (cy4q) binds selectively to thymine bulges in DNA and to a uracil bulge in RNA. Binding constants are in the low-micromolar range for thymine bulges in the stems of hairpins, for a thymine bulge in a DNA duplex, and for a uracil bulge in an RNA hairpin. Binding studies of Zn(cy4q) to a series of hairpins containing thymine bulges with different flanking bases showed that the complex had a moderate selectivity for thymine bulges with neighboring purines. The dissociation constants of the most strongly bound Zn(cy4q)−DNA thymine bulge adducts were 100-fold tighter than similar sequences with fully complementary stems or than bulges containing cytosine, guanine, or adenine. In order to probe the role of the pendent group, three additional zinc(II) complexes containing 1,4,7,10-tetraazacyclododecane (cyclen) with aromatic pendent groups were studied for binding to DNA including 1-(2-quinolyl)methyl-1,4,7,10-tetraazacyclododecane (cy2q), 1-(4-biphenyl)methyl-1,4,7,10-tetraazacyclododecane (cybp), and 5-(1,4,7,10-tetraazacyclododecan-1-ylsulfonyl)-*N*,*N*-dimethylnaphthalen-1-amine (dsc). The Zn(cybp) complex binds with moderate affinity but little selectivity to DNA hairpins with thymine bulges and to DNA lacking bulges. Similarly, Zn(dsc) binds weakly both to thymine bulges and hairpins with fully complementary stems. The zinc(II) complex of cy2q has the 2-quinolyl moiety bound to the Zn^{II} center, as shown by ^{1}H NMR spectroscopy and pH−potentiometric titrations. As a consequence, only weak (500 μM) binding is observed to DNA with no appreciable selectivity. An NMR structure of a thymine-bulge-containing hairpin shows that the thymine is extrahelical but rotated toward the major groove. NMR data for Zn(cy4q) bound to DNA containing a thymine bulge is consistent with binding of the zinc(II) complex to the thymine N3$^-$ and stacking of the quinoline on top of the thymine. The thymine-bulge bound zinc(II) complex is pointed into the major groove, and there are interactions with the guanine positioned 5′ to the thymine bulge.

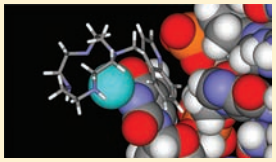

INTRODUCTION

Thymine bases in DNA are found in noncanonical Watson−Crick base pairs and in unpaired form in several important types of DNA structures. One of the most important of these structures is the DNA quadruplex, a four-stranded helical structure that forms in the telomeric ends of DNA.[1,2] Human telomeric DNA contains numerous TTAGGG repeats, and the thymine in these repeats is contained in loops between the G tetrads. Other important motifs include thymine−thymine base mismatches and thymine-containing hairpins that form in DNA-containing trinucleotide repeat sequences such as $(CAG)_n(CTG)_n$.[3−5] Such structures may disrupt DNA replication and have a central role in several human hereditary disorders. Thymine bulges constitute a third type of important DNA structural motif. Bulges either may form as intermediates in slipped DNA synthesis involving expanded DNA trinucleotide repeats or may arise during errors in replication.[6,7]

The recognition of such noncanonical structures in DNA by small molecules is an area of research that has attracted much attention over the past several years. It is extremely challenging to design small molecules that are capable of specifically targeting structures but potentially very rewarding to have in hand a set of compounds for modulating biological processes. However, despite the large number of biologically important DNA targets that contain thymine in noncanonical base pairs or in unpaired form, there are few molecules that specifically recognize these structures. In this study, we focus on metal-ion complexes that recognize single nucleotide thymine bulges in DNA as an alternative to the heterocyclic organic compounds that have been reported as recognition agents for thymine bases.[8−11]

Progress in the design of organic heterocyclic compounds has led to examples that bind with micromolar affinity to thymine bulges or mismatches, although selectivity over other nucleobases is not high. One of the most elegant approaches in the design of heterocycles for the recognition of thymine bulges is Nakatani's aglycone model for the pluaramycin antibiotic.[12] The model, because of its intercalative and alkylating properties, specifically alkylates a guanine that is opposite a thymine bulge. The unique reactivity of the thymine bulge toward this antibiotic leads to a high degree of specificity for bulged T's opposite a G. Nakatani and his group have designed additional heterocycles to bind to C/T bulges.[10] Another approach that relies on hydrogen-bonding complementarity features 2-ureidoquinoline, which has alternating acceptor−

Received: February 24, 2012
Published: April 16, 2012

dx.doi.org/10.1021/ic3004245 | *Inorg. Chem.* 2012, 51, 5444−5457

donor−donor hydrogen-bonding groups to facilitate binding and stabilization of single cytosine and thymine bulges in DNA.[13] Finally, a recently reported thymine-specific agent has a 7-deazaguanine group employed as a hydrogen-bonding group to pair with the nucleobase and an appended aromatic ring for stacking.[11] This compound exhibits micromolar binding and demonstrates 5-fold selectivity for T bulge over C bulge.

Metal-ion complexes have also been developed for bulge recognition. Most metal complex recognition agents for DNA bulges utilize inert metal ions for orientation of heteroaromatic ligands that stack onto the nucleobases to function through shape recognition. These complexes are generally not inherently specific for the type of base in the bulge. These include Barton's rhodium intercalators,[14,15] and nickel(II) and cobalt(II) macrocyclic complexes that are useful for probing bulged T, C, and A nucleobases through site-specific oxidation.[16] Dinuclear rhodium complexes with bipyridine- and bipyrimidine-derived ligands have been developed recently by Keene and co-workers to target the wider minor groove of single bulges in DNA.[17]

We recently communicated that a zinc(II) complex of 1,4,7,10-tetraazacyclododecane (cyclen) containing an aromatic pendent group [Zn(cy4q)], as shown in Figure 1, recognizes

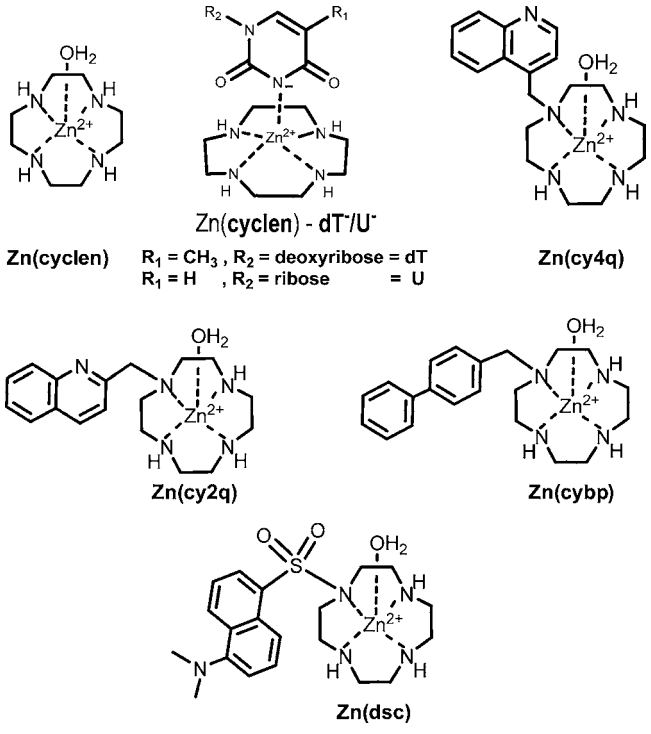

Figure 1. Zinc(II) macrocyclic complexes and Zn(cyclen) interaction with $N3^-$ of thymine.

DNA sequences containing a single thymine bulge with greater than 100-fold specificity over C, A, or G bulges and over otherwise identical sequences that lack a bulge.[18] Preliminary NMR spectroscopic studies were consistent with zinc(II) complex binding to the bulged thymine. Our work was motivated by the seminal studies of Kimura and his group, who explored Zn^{II}(cyclen) derivatives for the selective binding of thymine in single-stranded DNA.[19−21] Zinc(II) complexes of cyclen and other azamacrocycles bind to thymine and uracil by interaction of the Zn^{II} center with the deprotonated N3.[22,23] Hydrogen bonding between the cyclen amino groups and the thymine carbonyls was also proposed to be part of the recognition process. Work in our laboratory, however, showed a linear correlation between the magnitude of the hydroxide binding constant and that of the deprotonated thymine for a range of different zinc(II) macrocyclic complexes.[24] This shows that the Zn−$N3^-$ interaction, instead of hydrogen bonding, is the dominant interaction with thymine.

Kimura's work showed that certain macrocyclic zinc(II) complexes with pendent aromatic groups such as acridine bound selectively to thymine in single-stranded oligonucleotides.[21] In double-stranded DNA with AT-rich sequences, binding of zinc(II) macrocyclic complexes at relatively high ratios of complex to DNA-induced denaturation of the DNA.[25−27] Presumably, the zinc(II) complex binds to the Watson−Crick face of the thymine and disrupts the canonical base pairing in the duplex, leading to denaturation. While Kimura did not study thymines in unpaired or noncanonical DNA structures, his work showed that trinuclear and dinuclear zinc(II) complexes bound to the HIV-1 mRNA containing a trans-activation-responsive (TAR) structure. The TAR of HIV-1 mRNA has a three-nucleotide uracil bulge and normally binds to the HIV-1 regulatory protein Tat.[28] This seminal study, however, did not have molecular-level structural details on the binding of the multinuclear zinc(II) complexes to the bulge. In particular, it is of interest to know how binding of the zinc(II) complex changes the RNA structure, especially the structure of bases flanking the bulge, and whether binding affects the stability of the overall RNA structure. Our interest in the recognition of nucleic acid bulges leads us to explore whether zinc(II) macrocyclic complexes would selectively bind to and stabilize these secondary structures in RNA and DNA (Figure 2).[18] As shown here, the extrahelical nature of a thymine bulge in DNA makes the Watson−Crick face of the thymine

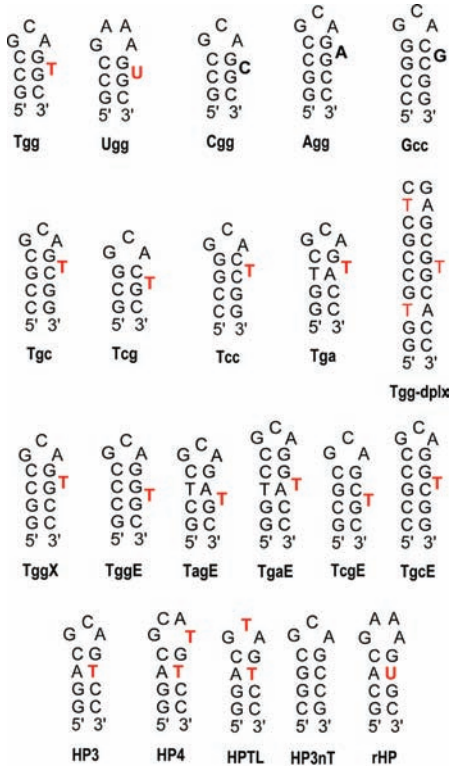

Figure 2. DNA and RNA hairpins and duplex.

dx.doi.org/10.1021/ic3004245 | Inorg. Chem. 2012, 51, 5444−5457

accessible for binding to the zinc(II) complex. This allows for moderate stabilization of the bulged structure by the zinc(II) complex and leads to unusually high selectivity for bulge recognition.

Here we present studies of thymine-bulge recognition with several zinc(II) derivatives of cyclen that contain different aromatic pendent groups to delineate the factors that are important in selective binding. NMR spectroscopy studies show that the thymine bulge within a hairpin is extrahelical. The Zn(cy4q) complex bound to the bulged thymine base has the quinoline stacked on the thymine and closely associated with the 5′-guanine in the major groove. These NMR structural studies are useful for gaining a better understanding of the specificity of the interaction of the Zn(cy4q) complex with bulged thymines in DNA.

EXPERIMENTAL SECTION

Materials and Methods. Cyclen condensation with glyoxal to yield the bridged macrocycle (perhydro-3,6,9,12-tetraazacyclopenteno-[1,3-*f*,*g*]acenaphthylene) proceeded as described with the addition done at 0 °C.[29] 1-(4-Quinolyl)methyl-1,4,7,10-tetraazacyclododecane (cy4q) was prepared as reported previously.[18]

$ZnCl_2$ was calibrated against a standardized solution of ethylenediaminetetraacetic acid using Eriochrome Black T as the indicator. Aqueous solutions for pH−potentiometric titrations were prepared from Milli-Q purified water that was degassed with nitrogen. Stock solutions of the ligands and complexes were standardized by ^{1}H NMR spectroscopy using the sodium salt of 3-(trimethylsilyl)-1-propanesulfonic acid.

DNA oligonucleotides were purchased from Integrated DNA Technologies (IDT) in desalted form. To ensure the removal of protecting groups, DNA from IDT was treated with fresh NH_4OH, with 1 mL added per 1 μmol of DNA. The solution was vortexed and kept in a water bath at 55 °C for 12 h. The NH_4OH solution was evaporated on a speedvac, and the sample was desalted through either isopropyl alcohol-induced precipitation, dialysis, or size-exclusion gel chromatography on a PD-10 column. Synthetic RNAs were purchased from Dharmacon in protected form and deprotected following their protocol. DNA for NMR studies was purchased from W. M. Keck Oligonucleotide Synthesis Facility (Yale University) as trityl-ON DNA oligonucleotides. Deprotection of the oligonucleotides was done by incubating the column-bound oligonucleotide with 2.0 mL of an ethanolic NH_4OH solution (mixture of 3 volumes of fresh 28−30% NH_4OH with 1 volume of 100% ethanol) at 55 °C for 12 h. The trityl-containing oligonucleotides were purified using a Glen-Pak cartridge using the protocol provided by Glen Research.

General Instrumentation. Thermo Orion ROSS pH 81152 (Thermo Electron, Inc.), coupled to a temperature compensation probe and a 702 SM Titrino (Metrohm) autotitrator was used for all pH and potentiometric measurements, respectively. ^{1}H NMR spectra were taken on an Inova 500 MHz NMR spectrometer; ^{13}C NMR spectra were recorded on a Gemini 300 MHz NMR spectrometer. A Beckman-Coulter DU-820 UV−vis spectrophotometer equipped with a high-performance Peltier temperature controller, a six-sample transport, and T_m package software was used for thermal denaturation studies and UV−vis experiments. Fluorescence measurements were obtained from a Varian Cary Eclipse fluorescence spectrophotometer equipped with Scan Software, version 1.1.

Synthesis of Macrocycles (See Also Figure SI-1 in the Supporting Information). 5-(1,4,7,10-Tetraazacyclododecan-1-ylsulfonyl)-N,N-dimethylnaphthalen-1-amine (dsc). This compound[30] was prepared by a route different from that previously reported. Dansyl chloride (1.038 g, 3.85 mmol) was dissolved in chloroform and slowly added, via an equalizing dropping funnel, to 5 mol equiv of 1,4,7,10-tetraazacyclododecane (cyclen; 3.324 g 19.3 mmol) in chloroform under N_2 at 0 °C. Once the dansyl chloride solution was added, the reaction mixture was allowed to stir at 0 °C for an additional 30 min. The crude reaction mixture was washed with H_2O twice, 1 N NaOH twice, and H_2O two more times. The organic layer was dried over anhydrous Na_2SO_4 and vacuum-dried to give a yellow oil. Yield: 90%. ESI-MS: m/z 406.3 (MH^+), 428.3 (MNa^+). ^{1}H NMR (500 MHz, $CDCl_3$, δ): 8.60 (d, 1 H, J = 9.0 Hz, Ar−*H*), 8.53 (d, 1 H, J = 9.0 Hz, Ar−*H*), 8.25 (d, 1 H, J = 6.5 Hz, Ar−*H*), 7.61 (t, 1 H, J = 7.2 Hz, Ar−*H*), 7.58 (t, 1 H, J = 7.0 Hz, Ar−*H*), 7.24 (d, 1 H, J = 7.0 Hz, Ar−*H*) 3.47 (t, 4 H, J = 5.0 Hz, NC*H*$_2$), 2.94 (s, 6 H, NC*H*$_3$), 2.85 (t, 4 H, J = 4.5 Hz, NC*H*$_2$), 2.82 (t, 4 H, J = 6.0 Hz, NC*H*$_2$), 2.68 (t, 4 H, J = 6.0 Hz, NC*H*$_2$). ^{13}C NMR (75 MHz, $CDCl_3$, δ): 151. 8, 133.7, 130.6, 130.5, 130.2, 130.1, 128.2, 123.2, 119.6, 115.2 (*C*−Ar), 49.9, 48.0, 47.4, 45.5 (*C*H$_2$N), 45.4 (*C*H$_3$N).

1-(Biphenyl)methyl−Cyclen−Glyoxal Bromide. To a solution of perhydro-3,6,9,12-tetraazacyclopenteno[1,3-*f*,*g*]acenaphthylene (**3** in Figure SI-1 in the Supporting Information;[29] 0.251 g, 1.30 mmol) dissolved in 1 mL of dry tetrahydrofuran (THF) was added a solution of 4-(bromomethyl)biphenyl (0.319 g, 1.30 mmol) in 0.5 mL of dried THF for 2−3 min. The mixture was stirred for 3 h at room temperature to form a white suspension. The suspension was centrifuged to collect the white solid. It was washed with cold THF and centrifuged at least three times further or until the centrifugate was clear and colorless. The solid was vacuum-dried to obtain a fine powder. Yield: 90%. ESI-MS: m/z 361.5 (MH^+). ^{13}C NMR (75 MHz, D_2O, δ): 142.52, 138.98, 133.07, 129.41, 128.57, 127.64, 127.02, 125.87 (*C*−Ar), 82.83, 71.71 (NCHN), 61.28, 60.96, 56.94, 51.34, 48.35, 48.20, 47.63, 47.57, 43.76 (*C*H$_2$N).

1-(4-Biphenyl)methyl-1,4,7,10-tetraazacyclododecane (cybp). To 0.168 g (0.500 mmol) of the alkylated salt 1-(biphenyl)methyl−cyclen−glyoxal bromide was added 1.0 mL of hydrazine monohydrate. The mixture was refluxed at 95 °C for 24 h and then extracted with hexanes (4 × 20 mL), followed by three more extractions of 50:50 $CHCl_3$/hexanes. Organic layers were combined, dried in Na_2SO_4, and vacuum-dried. The product was isolated by dropping in a 50:50 mixture of concentrated HCl and ethanol. The solids were washed with cold ethanol, centrifuged three times, and then vacuum-dried to yield a fine white powder. The free-base macrocycle was obtained by dissolving the solid in 3 mL of water, adjusting the pH to 12 with 3 M NaOH, and extracting with CH_2Cl_2. Yield: 40%. ESI-MS: m/z 339.3 (MH^+). ^{1}H NMR (500 MHz, $CDCl_3$, δ): 7.56 (dd, J = 18.5 and 7.9 Hz, 4H, Ar−H), 7.45−7.36 (m, 4H, Ar−H), 7.31 (dd, J = 16.0 and 8.6 Hz, 1H, Ar−H), 3.65 (s, 2H, ArC*H*$_2$), 2.85−2.77 (m, 4H, NC*H*$_2$), 2.72−2.66 (m, 4H, NC*H*$_2$), 2.64−2.55 (m, 8H, NC*H*$_2$). ^{13}C NMR (75 MHz, $CDCl_3$, δ): 141.57, 140.49, 138.57 (C−Ar), 129.94, 129.17, 127.62, 127.57 (CH−Ar); 59.44, 51.80, 47.66, 46.82, 45.61 (*C*H$_2$N).

1-(2-Quinolyl)methyl-1,4,7,10-tetraazacyclododecane (cy2q). A 5-fold excess (0.8614 g, 5 mmol) of cyclen was dissolved in 50.0 mL of previously dried CH_3CN in a 100-mL round-bottomed flask. The solution was maintained at 55−60 °C. 2-(Chloromethyl)quinoline hydrochloride (0.2141 g, 1 mmol) dissolved in dry CH_3CN was slowly added (1.5 h) to the cyclen solution using a dropping funnel. The mixture was refluxed for 12 h after the addition was complete. The reaction mixture was cooled to room temperature and the solvent evaporated. The residue was purified by silica gel chromatography using a gradient elution of 83% CH_2Cl_2/15% MeOH/2% NH_4OH. Yield: 65%. ESI-MS: m/z 314.3 (MH^+). ^{1}H NMR (500 MHz, D_2O, δ): 8.31 (d, J = 8.5 Hz, 1H, Ar−H), 7.93 (dd, J = 8.2 and 1.6 Hz, 2H, Ar−H), 7.79−7.74 (m, 1H, Ar−H), 7.60 (dd, J = 11.1 and 4.1 Hz, 1H, Ar−H), 7.44 (d, J = 8.5 Hz, 1H, Ar−H), 4.03 (s, 2H, C*H*$_2$−Ar), 3.01−2.89 (m, 16H, NC*H*$_2$). ^{13}C NMR (75 MHz, D_2O, δ): 159.66, 146.71, 138.44, 130.58, 128.30, 127.49, 127.06, 126.95, 121.23, (C−Ar), 59.00, 50.40, 44.85, 43.33, 43.18 (*C*H$_2$N).

[Zn(cy4q)]Cl$_2$. The free-base form of the cy4q ligand (40 mg, 0.13 mmol) was dissolved in a minimum amount of ethanol and added to 0.137 mmol of an ethanolic $ZnCl_2$ solution. The mixture was stirred for 1 h at room temperature. The fine powder was isolated, washed with cold ethanol, and dried in vacuo. Yield: 75%. ESI-MS: m/z 412.2 (100), 414.2 (87), 416.2 (55), 418.2 (14) ($[M - Cl^-]^+$); 189.9 (12) ($[(M - 2Cl^-)/2]^+$). ^{1}H NMR (500 MHz, D_2O, δ): 8.87 (d, J = 4.5 Hz, 1H, Ar−H), 8.29 (d, J = 8.5 Hz, 1H, Ar−H), 8.13 (d, J = 8.5 Hz,

dx.doi.org/10.1021/ic3004245 | *Inorg. Chem.* 2012, 51, 5444−5457

1H, Ar−H), 7.88 (t, J = 7.6 Hz, 1H, Ar−H), 7.76 (t, J = 7.7 Hz, 1H, Ar−H), 7.62 (d, J = 4.5 Hz, 1H, Ar−H), 4.57 (s, 2H, CH_2−Ar), 3.27−2.77 (m, 2H), 3.01−2.88 (m, 8H, NCH_2), 2.88−2.77 (m, 4H, NCH_2), 2.72 (ddd, J = 13.4, 7.3, and 3.5 Hz, 2H, NCH_2).

[Zn(cybp)]Cl$_2$. The free-base form of the cybp ligand (30 mg, 0.09 mmol) was dissolved in a minimum amount of ethanol, and to this was added to 0.095 mmol of an ethanolic $ZnCl_2$ solution. The mixture was stirred for 1 h at room temperature. The fine white solid was isolated, washed with cold ethanol, and dried in vacuo. If no solid precipitated, the solvent was evaporated and the complex was recrystallized in ethanol. Yield: 80%. ESI-MS: m/z 437.3 (100), 439.2 (90), 441.2 (60) ($[M - Cl^-]^+$); 401.3 (29), 403.2 (23), 405.2 (13) ($[(M - 2Cl^- - H^+]^+$). ^{1}H NMR (500 MHz, D_2O, δ): 7.74 (dd, J = 12.3 and 7.8 Hz, 4H, Ar−H), 7.55 (t, J = 7.6 Hz, 2H, Ar−H), 7.52−7.44 (m, 3H, Ar−H), 4.06 (s, 2H, CH_2−Ar), 4.02 (s, 2H, NCH_2), 3.23 (d, J = 3.9 Hz, 2H, NCH_2), 3.03−2.94 (m, 4H, NCH_2), 2.93−2.78 (m, 8H, NCH_2).

[Zn(cy2q)]Cl$_2$. The same procedure that was used to obtain [Zn(cybp)]Cl_2 was followed. Yield: 70%. ESI-MS: m/z 376.1 (75), 378.2 (41), 380.2 (30) ($[(M - 2Cl^- - H^+]^+$); 189.0 (100), 190.0 (64), 191.0 (45) ($[(M - 2Cl^-)/2]^+$). ^{1}H NMR (500 MHz, D_2O, δ): 8.53 (d, J = 8.5 Hz, 1H, Ar−H), 8.26 (d, J = 8.5 Hz, 1H, Ar−H), 8.02 (d, J = 8.1 Hz, 1H, Ar−H), 7.85 (dt, J = 17.6 and 8.6 Hz, 2H, Ar−H), 7.73−7.64 (m, 1H, Ar−H), 7.53 (dd, J = 12.0 and 4.8 Hz, 1H, Ar−H), 7.35 (d, J = 8.5 Hz, 1H, Ar−H), 4.36 (s, 1H, NCH_2), 4.07 (s, 1H, NCH_2), 3.21−2.68 (m, 18H, NCH_2).

[Zn(dsc)]Cl$_2$. The same procedure that was used to obtain [Zn(cy4q)]Cl_2 was followed. The resulting fine yellow powder was vacuum-dried. Yield: 74%. ESI-MS: m/z 504.2 (100), 506.2 (91), 508.1 (57) ($[M - Cl]^+$); 236.2 (10) ($[(M - 2Cl^-)/2]^+$). ^{1}H NMR (500 MHz, D_2O): 8.51 (d, 1 H, J = 8.5 Hz, Ar−H), 8.45 (d, 1 H, J = 8.5 Hz, Ar−H), 8.21 (d, 1 H, J = 7.0 Hz, Ar−H), 7.65 (t, 1 H, J = 8.0 Hz, Ar−H), 7.59 (t, 1 H, J = 8.2 Hz, Ar−H), 7.33 (d, 1 H, J = 8.0 Hz, Ar−H), 3.56 (m, 2 H, J = 11.0 Hz, NCH_2), 3.50 (m, 2 H, J = 7.2 Hz, NCH_2), 3.19 (t, 2 H, J = 13.5 Hz, NCH_2), 2.93 (m, 4H, NCH_2), 2.76 (s, 6H, NCH_3), 2.68 (m, 2H, NCH_2). ^{13}C NMR (75 MHz, D_2O, δ): 152.0, 132.6, 131.9, 130.0, 125.7, 124.3, 119.0, 115.9, 110.0 (C−Ar), 47.6, 46.5, 45.5 45.0 (CH_2N), 44.3 (CH_3N).

pH−Potentiometric Titrations. Potentiometric−pH titrations of ligands in the absence and presence of $ZnCl_2$ were conducted using a Brinkmann Metrohm 702 SM Titrino autotitrator equipped with temperature compensation and a Thermo Orion ROSS pH 81152 electrode. A carbonate-free solution of 0.100 M NaOH was prepared and standardized using potassium hydrogen phthalate and phenolphthalein as indicators. HCl (0.100 M) was standardized using borax ($Na_2B_4O_7{\cdot}10H_2O$) with methyl orange as the indicator. The electrode was initially calibrated as a hydrogen concentration probe by titrating known amounts of the standardized HCl with the standardized NaOH. The program *GLEE* was used to calculate the standard electrode potential and the carbonate content of the NaOH solution.

Solutions of the fully protonated ligand (0.5−1.0 mM) with and without 1.05 equiv of Zn^{2+} were titrated with the standardized NaOH up to pH 11 at 25 °C with I = 0.100 M NaCl under argon atmosphere. The volume of the added increment was set at 0.02 mL and the equilibration time set to 60 s (ligand) or 240 s (ligand and $ZnCl_2$). At least two independent titrations were done for each system. The program *HYPERQUAD 2008* was used to calculate the protonation and stability constants from the pH data.[31] The K_w (=$[H^+][OH^-]$) or ionic product of the water value used for these experimental conditions (I = 0.10 M NaCl, 25 °C) was $10^{-13.77}$. The least-squares fits of the calculated/model-derived points to the observed values were satisfactory, with the average statistical parameter, σ, in the acceptable 1.3−3.4 range. Speciation diagrams, plotted as a percent formation against pH, were constructed through the free program *HYSS*.

Optical Thermal Denaturation Studies. Solutions containing the oligonucleotide and 50 mM NaCl were annealed by heating to 90−95 °C for 5−10 min, followed by slow cooling to room temperature. Oligonucleotide stock solution concentrations were obtained spectrophotometrically at 25 °C using molar extinction coefficients for each oligonucleotide at 260 nm. Optical thermal melting experiments were carried out with DNA concentrations that differed by at least 10-fold. Melting temperatures (T_m) were obtained by fitting the data to the *Meltwin* 3.5 program available at http://www.meltwin3.com/.[32]

The optical thermal melting profiles of the oligonucleotides were studied in the presence of up to 3 equiv of the zinc(II) macrocyclic complex to a DNA solution composed of 0.020 M HEPES, pH 7.5, and 0.10 M NaCl.

Fluorescence Spectroscopy Measurements. For ethidium bromide (EtBr) fluorescence displacement assays, a stock solution of EtBr was standardized using ε = 5600 L/mol·cm at 480 nm.[33−35] The procedure used by Boger et al.[36] was followed with minor modifications. Blank solutions were composed of 2 mL of 0.10 M NaCl, 0.020 M HEPES, and pH 7.5 with 4.4 μM EtBr concentration. The fluorescence of this solution was subtracted from that of identical solutions containing DNA and a metal complex. Solutions for fluorescence displacement measurements contained 8.8 μM DNA base pairs. Excitation was measured at 545 nm, and emission was monitored from 565 to 700 nm with a scan rate of 120 nm/min. A concentrated aqueous stock solution of the zinc(II) complex was added, and the solution was mixed and incubated for 5 min prior to the reading.

The binding curves were generated for the signal at an emission maximum of 605 nm. The concentration of the binding agent was plotted versus the difference of the fluorescence signal in the absence and presence of the zinc(II) complex. The curve was fit as previously reported to equations for both competitive and noncompetitive binding.[18] All data for fluorescence displacement assays were fit to eq (1), which has been further developed for multisite binding.[37] Here I is the fluorescence intensity, Φ represents the fluorescence intensity upon saturation of DNA binding sites with ligand, $K_{d(app)}$ is the apparent dissociation constant, and $[S]_T$ represents the total DNA concentration in solution. $[L]_f$ and $[L]_T$ are the free and total ligand concentrations in solution, respectively.

$$I = \phi\left(\frac{[L]_f}{K_{d(app)} + [L]_f}\right)$$

$$[L]_f = 0.5(-b + \sqrt{b^2 + 4[L]_T + K_{d(app)}})$$

$$b = [S]_T - [L]_T + K_{d(app)} \quad (1)$$

Intrinsic dissociation constants were obtained from apparent dissociation constants and measured EtBr binding constants, as shown in eq 2. Binding constants for EtBr to a thymine-containing DNA bulge, a uracil bulge, and for DNA and RNA duplexes are repectively as follows: $K_{EtBr(DNA\ bulge)}$, 1.33×10^5; $K_{EtBr(U\ bulge)}$,[38] 8.00×10^5; $K_{EtBr(DNA\ stem)}$,[39] 7.41×10^4; $K_{EtBr(RNA\ stem)}$,[39] 1.32×10^4 M^{-1}.

$$K_d = K_{d(app)}/K_{EtBr}[EtBr] \quad (2)$$

Fluorescence spectra obtained with 10 μM Zn(dsc) were obtained in a 0.020 M HEPES buffer adjusted to a pH of 7.5 and 0.10 M NaCl. The sample was excited at 335 nm, and emission of the dansyl fluorophore was measured from 430 to 630 nm. The fluorescence intensity of the solution was plotted as a function of the DNA concentration. In this case, both the bound and free Zn(dsc) are fluorescent and the fluorescence of the free Zn(dsc) was not subtracted out. This made it necessary to use a 1:1 binding equation with parameters for two fluorescent species (eq 3). In eq 3, $[L]_B$ represents bound Zn(dsc). X_{LB} and X_L are the mole fractions of bound Zn(dsc) and free Zn(dsc), respectively, and I_{LB} and I_L are the fluorescence emission intensities of bound Zn(dsc) and free Zn(dsc), respectively.

$$[L]_B = 0.5[K_{d(app)} + [L]_T + [S]_T - \sqrt{(K_{d(app)} + [L]_T + [S]_T)^2 - (4[L]_T[S]_T)}]$$

$$I = X_{LB}I_{LB} + X_LI_L \quad (3)$$

NMR Spectroscopy. Deprotected, purified, and lyophilized DNA samples were redissolved in 500 μL total volume of 99.96% D_2O (nonexchangeable proton experiments) or 90% H_2O/10% D_2O

dx.doi.org/10.1021/ic3004245 | Inorg. Chem. 2012, 51, 5444−5457

Table 1. Ligand Protonation (log K) and Zn^{II} Binding Constants (log K_{Zn}) at 25 °C, 0.10 mM NaCl

equilibria	cyclen[a]	cy4q[b]	cybp	cy2q	dsc
Ligand					
log K_1	11.04; 10.7	9.89 ± 0.02	11.33 ± 0.22	10.70 ± 0.03	9.46 ± 0.25
log K_2	9.86; 9.70	7.91 ± 0.02	8.76 ± 0.20	9.15 ± 0.04	6.44 ± 0.03
log K_3	<2; <2	4.24 ± 0.03	3.10 ± 0.32	2.89 ± 0.05	3.66 ± 0.07
log K_4	<2; <2	<2	<2	<2	2.42 ± 0.21
log K_5		<2		<2	<2
Metal Complex					
log K_{Zn}	15.74; 16.2	11.42 ± 0.04	13.28 ± 0.09	14.42 ± 0.02	10.93 ± 0.1
log K_{ZnLH}		4.94 ± 0.07	5.88 ± 0.13	5.54 ± 0.02	5.78 ± 0.2
pK_a (Zn−OH_2)	8.28; 7.88	8.30 ± 0.06	8.49 ± 0.14	11.22 ± 0.06	7.92 ± 0.1

[a]From refs 21 and 22. [b]From ref 18.

(exchangeable proton experiments) with 0.10 M NaCl and 0.020 M HEPES, pH 7.5. At least two more rounds of redissolving and redrying were carried out. The lyophilized sample was then resuspended in 500 μL of solvent and annealed by heating of their solution up to 90−95 °C for 5−10 min, followed by slow cooling (8−12 h) to room temperature. The oligonucleotide concentration (1−2 mM) was obtained spectrophotometrically at 25 °C using a molar extinction coefficient for each oligonucleotide at 260 nm.

^{1}H NMR spectra were obtained on a Varian Inova 500 MHz NMR equipped with a triple-resonance probe at 25 °C. Spectra were processed and analyzed using Varian *VNMRj* software or *MestReNova*, version 6.2.1−7569 (MestRelab SL), software. The one-dimensional (1D) experiments consisted of 64 transients per free induction decay with 17650 data points and 3 s recycle delay. The chemical shifts were referenced to the HDO signal (4.8 ppm at 25 °C). Presaturation of the water peak was used to reduce the size of the HDO peak. 1D NMR data was apodized with either (0.7−1 Hz) line broadening or shifted sine-bell apodization.

1D exchangeable imino proton spectra were collected at 5 or 10 °C using either WATERGATE[40] solvent suppression or 1−1 spin−echo NOESY (rna_11NOESY pulse sequence, n_i = 1)[41] pulse sequences with 4096 data points, 64 transients, and 1 s recycle delay. The maximum hertz offset was 5000 Hz for the 1−1 spin−echo NOESY, giving maximum excitation at 14.8 ppm. NMR data was apodized with (0.7−1 Hz) line broadening or shifted sine-bell apodization. Exchangeable and nonexchangeable two-dimensional (2D) spectra were collected at 25 or 15 °C. They were processed and analyzed using Varian *VNMRj* software. Experiments were collected using a 2.0 s recycle delay and in-phase-sensitive mode. All 2D spectra were apodized with either sine-bell and shifted sine-bell functions in both dimensions.

With the standard NOESY[42] pulse sequence, spectra were collected with mixing times of 0.10, 0.15, 0.20, and 0.40 s with the water peak applied with a presaturation pulse for 0.25 s. Experiments were run with a spectral width of 4406 Hz, 4K data points, 32 transients, and 256 increments. Data set in t1 dimension was zero-filled to obtain a 4K × 4K matrix.

Total correlation spectroscopy (TOCSY)[43,44] experiments were obtained using the standard pulse sequence with the same spectral width, data points, and increments as the NOESY experiment but with the number of transients collected at 32 or 48. Double-quantum filtered-correlation spectroscopy (DQF-COSY)[45,46] spectra were collected using the standard pulse sequence with the same spectral width, data points, and transients as the NOESY experiment but with the number of increments set to 512.

Molecular Modeling. Sparky[47] was used to assign peaks and measure peak volumes for distance restraints, and CYANA-2.1[48,49] was used to calculate the structures using NMR distance restraints. Discovery Studio Visualizer, version 2.5 (Accelrys Software, Inc.), was used to render the three-dimensional (3D) structures.

Distance restraints were obtained using a Gaussian fit of individual peaks from a 150 ms NOESY spectrum with each peak integrated and its volume calculated. The volume of the C−H5/H6 cross peaks was used to determine the distance between protons using the isolated spin-pair approximation (ISPA). Upper and lower bound distance restraint values were set to ±20% of the ISPA-determined distances, as indicated by NOEs observed in nonexchangeable 2D NMR spectra. The standard CYANA-2.1 Watson−Crick base-pairing restraints were generated for the base pairs in the stem and G(N3)−A(N6) and G(N2)−A(N7) restraints for the sheared GA mismatch. A total of 81 NOE restraints and 23 hydrogen-bonding/base-pairing restraints were used for Tgg:Zn(cy4q) calculations and 118 NOE and 32 hydrogen-bonding/base-pairing restraints for the TggX calculations. For the Tgg:Zn(cy4q) structure, the Tgg hairpin structure was determined without the zinc(II) complex using CYANA-2.1 and the Zn(cy4q) docked to this structure.

For each hairpin structure, CYANA-2.1 was used to calculate 1000 structures using the standard 'calc_all' protocol, and the top 20 structures that best fit the NMR data (lowest F number) were analyzed. NOE restraints and distance restraints from CYANA calculations are provided in the Supporting Information.

HyperChem 6.0 was used to dock the Zn(cy4q) ligand to one of the Tgg structures. A Tgg structure that allowed Zn(cy4q) q-H3 and q-H8 to be near the G8 sugar with no steric interactions between the cyclen moiety and the major groove was selected. Zn(cy4q) was constructed in *HyperChem* and then energy-minimized prior to docking. The H3 proton was removed from T9 and Zn(cy4q) positioned with Zn^{II}(cyclen) at the hydrogen-bonding face of T9 with the Zn^{II} ion located near the N3 of T9. All of the nucleotides in the Tgg structure were fixed in space except for T9 and the flanking G8:C4 and G10:C3 base pairs. The complex was then energy-minimized to eliminate steric interactions from docking.

Further information on NOE and distance restraints from CYANA calculations is listed at the end of the Supporting Information. The structures were deposited in the PDB (entries 2LO5, 2LOA, and 2LO8).

RESULTS

Solution Chemistry of Zinc(II) Macrocyclic Complexes.

To characterize zinc(II) macrocyclic solution chemistry, pH−potentiometric titrations were carried out on the macrocyclic ligands with and without $ZnCl_2$ (I = 0.10 M NaCl, 25 °C; Figure SI-2a−c in the Supporting Information). Fitting data to equilibria (eqs S1−S16 in the Supporting Information) gave the ionization constants of the ligands, the equilibrium binding constant of the neutral ligand with the Zn^{II} ion, and an ionization constant for loss of the proton from the zinc(II) complex at high pH, presumably for the formation of a zinc(II) hydroxide complex.

Data showing stepwise protonation of the ligands (log K_{1-4}) and the formation constants for Zn metal (log K_{Zn}) of the four zinc(II) complexes along with data for the unsubstituted cyclen ligand for comparison are summarized in Table 1. In all macrocyclic ligands (Figure 1), the fully protonated cyclen

dx.doi.org/10.1021/ic3004245 | *Inorg. Chem.* 2012, 51, 5444−5457

group has two weakly basic and two strongly basic amines. The weakly basic groups ionize at a pH too low (<2) to be accurately determined, whereas protonation of the two strongly basic amines is modulated by the pendent aromatic groups to give protonation constants ranging from 7.9 to 11.3. For the quinoline pendant cyclen macrocycles, the quinoline nitrogen protonation constants are 4.24 ± 0.03 and 2.89 ± 0.05 for 4-methylquinoline and 2-methylquinoline, respectively. These constants are comparable to previously reported values for similar ligands.[21,50] The dansyl group has a pK_a of 3.66, close to that anticipated for the dimethylamino group.[51]

In the presence of 1 equiv of Zn^{II}, three distinct deprotonation events in the pH range 2.5−10.0 for Zn(dsc), Zn(cybp), and Zn(cy2q) were observed. These correspond to deprotonation of the cyclen ring upon formation of the Zn^{2+} complex to form Zn(L) and Zn(LH) (L = macrocycle) and deprotonation of the Zn^{II}-bound water to form a zinc(II) hydroxide complex. As reported previously, Zn(cy4q) also shows three ionization events.[18] The macrocyclic complex Zn(LH), which exists at acidic pH values, has a site of protonation that may be on the nitrogen of either the quinoline, dansyl group, or macrocycle. All macrocycles with pendent aromatic groups bind Zn^{II} with high affinity, as shown by the large binding constants (log K_{Zn} = 11.4−14.4), although binding is not as strong as that for Zn(cyclen) (log K_{Zn} = 16.0). The lowest value of K_{Zn} belongs to the Zn(dsc) complex. This weaker binding is attributed to the participation of one of the macrocyclic amine lone pairs in bonding to the sulfone, giving this complex a formation constant closer to that of a triazacyclononane macrocycle.[24,52]

The pK_a values of the zinc(II) water ligands of Zn(cy4q), Zn(cybp), and Zn(dsc) are 8.3, 8.5, and 7.9, respectively. These values are comparable to those of analogous zinc(II) macrocyclic complexes determined in the presence of a 0.10 M chloride anion.[24] In contrast, the pK_a of the Zn(cy2q) complex is at an exceptionally high value of 11.2, which is attributed to binding of the 2-methylquinoline group to the Zn^{II}, leading to suppression of the formation of the zinc(II) hydroxide complex. Binding of macrocyclic amines and the 2-methylquinoline pendent group is confirmed by a ^{1}H NMR titration of the cy2q ligand with Zn^{II}, as shown in Figure SI-2d in the Supporting Information. Data show that adding Zn^{II} to the macrocycle leads to new aromatic ring resonances and to splitting of the methylene linker resonance at 4.08 ppm into two resonances at 4.14 and 4.43 ppm.

Speciation diagrams generated from the titration data using the program *HySS* are shown in Figure SI-2e−h in the Supporting Information for solutions containing 1.00 mM Zn^{II} and ligand. Four major zinc(II) species are present including the free Zn^{II} ion, the tricationic zinc(II) complex with a monoprotonated ligand $[(Zn(LH)]^{3+}$, the dicationic zinc(II) complex with bound water ($[(Zn(L)(OH_2)]^{2+}$), and the zinc(II) hydroxide complex ($[Zn(L)(OH)]^{+}$). The large affinity of the macrocycle for the Zn^{II} ion ensures that most of the Zn^{II} ion is already bound by the macrocycle at pH < 5. It is noteworthy that the dicationic zinc(II) complex ($[Zn(L)(OH_2)]^{2+}$), the species that binds thymine or uracil groups, predominates in >70% at the pH (7.5) used in the studies here for all of the complexes at 1.00 mM concentrations of ligand and $ZnCl_2$. Speciation diagrams were also generated for solutions of the complexes containing 100, 10, and 1 μM Zn^{II} and ligand as representative concentrations used in fluorescence titrations. These data show that Zn(cy4q), Zn(dsc), and Zn(cybp) exist predominantly as the dicationic Zn(L) complex at pH 7.5 even at micromolar concentrations (≤2.5% free Zn^{II} at 10 μM; Table S1 in the Supporting Information). Table S1 in the Supporting Information shows that Zn(dsc) has a slightly higher percentage of the hydroxide complex present at pH 7.5 in comparison to the other two complexes as anticipated from the lower pK_a of the bound water (Table 1).

DNA Binding. Of the four complexes studied here, only the Zn(dsc) complex has fluorescence properties that are useful for direct DNA binding studies (Figure SI-3 in the Supporting Information). Studies on several simple unstructured oligonucleotides including AAAAA, AATAA, CCCCC, and CCTCC (Table 2) showed that only the thymine-containing oligonucleotides, AATAA and CCTCC, bound the Zn(dsc) complex with micromolar dissociation constants. Weak binding of Zn(dsc) with only a very small change in fluorescence ($K_{d(app)}$ > 200 μM for CCCCC and > 1000 μM for AAAAA) was observed for oligonucleotides not containing thymine. Previously reported binding constants for Zn(dsc) to oligonucleotides differ from those reported here,[53] but these studies were carried out under different buffer conditions with low concentrations (1 μM) of Zn(dsc). For comparison with Zn(dsc), binding of Zn(cy4q) to CCTCC was studied by using UV−vis spectroscopy. A dissociation constant of 25 μM was obtained, very similar to values obtained for this complex with thymine.[54] Monitoring the binding of Zn(cybp) to single-stranded DNA was not feasible because of a lack of fluorescence or UV−vis properties that can be readily distinguished from those of DNA.

Table 2. Apparent Dissociation Constants ($K_{d(app)}$, ×10^{-6} M)[a] of Zinc(II) Macrocyclic Complexes

complex	Zn(cy4q)b	Zn(cybp)	Zn(cy2q)	Zn(dsc)
CCTCC	25[b]	nd	nd	55
AATAA	nd	nd	nd	50
Tgg	2.2 ± 0.2[c]	9 ± 2[d]	171 ± 25	250 ± 34
Ugg	12 ± 3[c]	285 ± 58	334 ± 47	nd
Cgg	185 ± 40[c]	nd	nd	nd
Agg	>200[c]	nd	nd	nd
Gcc	108 ± 1[c]	nd	nd	nd
HP3	142 ± 50[c]	93 ± 18	427 ± 77	>1000
HP4	104 ± 22	79 ± 21	193 ± 91	nd
HPTL	127 ± 16[c]	75 ± 26	459 ± 35	>1000
HP3nT	435 ± 10	118 ± 7	421 ± 56	nd
rHP	20 ± 2	102 ± 14	299 ± 64	nd

[a]Apparent dissociation constants from nonlinear fitting to eq 1 for all complexes except Zn(dsc) in 0.10 M NaCl, 0.020 M HEPES, pH 7.5, [EtBr] = 4.4 μM, [oligonucleotide] = 8.8 μM in base-pair data for Zn(dsc) were fit to eq 3. [b]From UV−vis spectroscopic titration. [c]From ref 18. [d]From an increase in EtBr fluorescence upon the addition of a zinc(II) complex. nd = not determined.

A panel of hairpin loops with single base bulges or with fully complementary stems was used to study the binding preferences of the zinc(II) complexes. The strongly hairpin-nucleating 5′-GCA-3′ or 5′-GAAA-3′ loops were used for DNA and RNA, respectively. The hairpin structure for these oligonucleotides is supported by the lack of a concentration dependence of the T_m values over the concentration range 1.0−15 μM at pH 7.5, 0.10 M NaCl, and 0.020 M HEPES, in support of a unimolecular process. As shown in Table SI-2 in

dx.doi.org/10.1021/ic3004245 | Inorg. Chem. 2012, 51, 5444−5457

the Supporting Information, hairpins lacking a bulge such as HP4 have T_m values that are quite high (70.6 °C), but the presence of a bulged base clearly destabilizes the hairpin, with more prominent effects on hairpins with only three base pairs such as Tgg. Thus, Tgg and Tgc have T_m values of 53 and 68 °C, respectively (Table SI-2 in the Supporting Information). In addition, a duplex containing a single thymine bulge, Tgg-dplx, was studied.

Direct monitoring of the quinoline or biphenyl fluorescence of Zn(cy4q), Zn(cy2q), or Zn(cybp) was not possible because of interference with the DNA optical properties, so an EtBr fluorescence displacement assay was used to monitor binding.[36] EtBr increases its fluorescence by as much as 20-fold when it binds to DNA.[55] In this displacement assay, fluorescent DNA-bound EtBr is titrated with the DNA binding agent, and the decrease in fluorescence due to EtBr displacement as a function of the added binding agent is monitored. This approach works well in cases where EtBr binds to the oligonucleotides in a 1:1 stoichiometry and within the vicinity of the binding site of the ligand. Studies showed that EtBr bound to hairpins with a minimum of four base pairs, most likely to an ApC step or a CpG step for motifs with purely CG base pairs, corresponding to the selectivity of EtBr for alternating purine−pyrimidine bases.[56−60] On the other hand, EtBr binds to a bulged stem with only three base pairs, consistent with an enhanced affinity of EtBr binding to bulged oligonucleotides in comparison to a regular duplex.[38,61] EtBr binding has no pronounced preference for bulged base identity or sequence; the essential feature of the bulges is the extra sugar−phosphate unit in the helix, which renders the backbone flexible enough to adapt to a new conformation when EtBr intercalates. The exact binding site for EtBr in bulged DNA has been proposed to be either one base pair away from the bulge[61] or two base pairs removed from the bulge.[62] Binding of the complexes to the bulged DNA is thus expected to displace the proximate EtBr. As shown below, this is indeed the case for most hairpins, with a few exceptions that show that the zinc(II) complex apparently enhances binding of EtBr, as shown by an increase in fluorescence upon the addition of the zinc(II) complex.

Single-site binding of EtBr was supported by a series of Job's plots for representative motifs (Figure SI-4 in the Supporting Information) that show the strong inflection at ∼0.5 corresponding to a 1:1 binding ratio between EtBr and a hairpin oligonucleotide. Control experiments also showed that the fluorescence intensity of the DNA−EtBr adduct does not decrease over time, nor does a representative zinc(II) complex, Zn(cy4q), quench the fluorescence (Figure SI-5 in the Supporting Information).

In Table 2 are listed the apparent dissociation constants determined from the nonlinear fitting of the data to a 1:1 binding model (eq 1) for fluorescence displacement assays[37] or to eq 3 for direct fluorescence assays. Intrinsic dissociation constants derived from a competitive binding model (eq 2)[63,64] based on EtBr binding constants to DNA are included for representative oligonucleotides in Table 3.

The data in Table 2 show that Zn(cy2q) binds weakly and with low selectivity with apparent binding constants ranging from 100 to 400 μM. Even with the addition of a 100 μM Zn(cy2q) complex, very low displacement fractions (0.3 out of 1) of EtBr were observed compared to the other complexes (Figure SI-6 in the Supporting Information). Unlike the other complexes, Zn(cy2q) has no open coordination site; thus, its lack of selectivity, and weak binding is consistent with the absence of an available coordination site for binding of the thymine/uracil anion. Binding to the DNA is likely driven by the cationic charge of the complex, which leads to similar binding constants for all oligonucleotides.

Table 3. Dissociation Constants for Zn(cy4q) Binding to Oligonucleotides

motif	$K_{d(app)}$[a] (×10^{-6} M)	K_d[b] (×10^{-6} M)
Tgg	2.2 ± 0.2	3.8
Ugg	12 ± 3	3.4
Cgg	185 ± 40	315
Gcc	108 ± 1	184
Agg	>200	>400
Tgc	1.2 ± 0.8	3.4
Tcg	3.8 ± 1.4	6.5
Tcc	22.2 ± 0.2	37.8
Tga	1.3 ± 0.1	2.2
TggX	1.2 ± 0.4	2.1
TggE	1.4 ± 0.4	2.4
TagE	3.2 ± 0.3	5.4
TgaE	2.0 ± 0.2	3.4
TcgE	2.2 ± 1.4	3.8
TgcE	5.5 ± 0.3	9.4
Tgg-dplx	1.5 ± 0.1	2.6
HP3	142 ± 50	435
HP3nT	435 ± 10	1334
rHP	20 ± 2	343

[a]Apparent dissociation constant from fitting to eq 1 for solutions containing 0.10 M NaCl, 0.020 M HEPES, and pH 7.5. [b]$K_d = K_{d(app)}/K_{EtBr}[EtBr]$; $K_{EtBr(DNA\ bulge)} = 1.33 \times 10^5$; $K_{EtBr\ (U\ bulge)}$[38] $= 8.00 \times 10^5$; $K_{EtBr\ (DNA\ stem)}$[39] $= 7.41 \times 10^4$; $K_{EtBr\ (RNA\ stem)}$[39] $= 1.32 \times 10^4$ M^{-1}.

Neither Zn(cybp) nor Zn(dsc) have pendent planar aromatic groups that are optimal for forming stacking interactions with DNA. As a consequence, neither complex shows good selectivity for thymine bulges. Zn(cybp) has a nonconjugated biphenyl pendant aromatic group and shows little selectivity for binding to the different oligonucleotides. It has the strongest apparent affinity for Tgg with a dissociation constant of 9 μM. However, this binding of Zn(cybp) to the EtBr-bound Tgg promotes an increase in EtBr fluorescence rather than the expected decrease that occurs upon displacement of EtBr from the DNA. This increase in EtBr fluorescence may result from a change in the orientation and stacking of EtBr in the DNA that occurs upon binding of Zn(cybp) to the DNA. It is then difficult to compare the binding constants obtained from retention of EtBr to those resulting from EtBr displacement because binding of the Zn(cybp) complex may be influenced by the presence of the DNA-bound EtBr.

Similar to Zn(cybp), Zn(dsc) has an aromatic group that is not entirely planar because of the exocyclic dimethylamino group that rotates[65] out of the plane of the ring and a sulfone group that is less flexible than the methylene group connecting the pendent aromatic. Zn(dsc) does not bind strongly to DNA bulges or hairpins lacking bulges.

Zn(cy4q) has appended 4-quinoline, a planar electron-deficient aromatic group that is favorable for stacking on the nitrogenous bases of DNA or RNA.[66] This complex also has a relatively flexible methylene group as a linker and the quinoline nitrogen positioned so that it cannot bind to the Zn^{II} center. Apparent dissociation constants from EtBr displacement are given in Table 2, and intrinsic dissociation constants (K_d), obtained after taking into account the binding of EtBr to

dx.doi.org/10.1021/ic3004245 | Inorg. Chem. 2012, 51, 5444−5457

representative oligonucleotides, are given for additional bulges in Table 3 by using eq 2. Binding to thymine bulges is selective with a 400-fold difference in the K_d values for the oligonucleotides studied here (Table 3). Zn(cy4q) binds to all of the motifs, except Tgc, through displacement of EtBr with a corresponding decrease in the fluorescence signal. Apparent binding constants show a preference for thymine and uracil in bulges, Tgg and Tgc (K_{app} = 2 μM), followed by the uracil bulge (Ugg). Zn(cy4q) has 400-fold tighter apparent binding to a thymine bulge in a hairpin structure compared to an analogous hairpin lacking a bulge (compare TggX to HP3nT). There is a 50−100-fold preference for thymine-containing bulges compared to analogous C, G, or A bulges. Zn(cy4q) binds to a uracil bulge within a RNA hairpin (Ugg) about 6-fold less tightly than to DNA thymine bulges. However, if the tighter binding of EtBr to RNA bulges in comparison to DNA bulges is taken into account in a competitive binding model to obtain K_d, Zn(cy4q) is bound to the RNA bulge nearly as tightly as to the DNA bulge (Table 3).

Given the apparent preference for binding of Zn(cy4q) to thymine bulges, we further studied additional thymine bulges with different flanking bases. The tightest binding affinities are observed for motifs with two purines as flanking bases (Tgg, TggE, Tga, TgaE, and TagE). With two cytosines as flanking bases (Tcc), the binding constant was 10-fold weaker than that for bulges with flanking purines. A similar trend of reduced affinity can be observed for the motif with a cytosine at the 3′ side of the thymine bulge (TgcE). Notably, the addition of an extra CG base pair between the GCA loop and the 5′ flanking base pair of the bulge (e.g., Tgg vs TggE, Tga vsTgaE, and Tcg vs TcgE) does not markedly change the binding affinity of the complex, suggesting that the complex interacts with the thymine bulge locally, without key interactions involving the loop nucleotides. This was confirmed by a study of the duplex, Tgg-dplx, containing thymine bulges, which also gave micromolar binding constants. Intrinsic dissociation constants (K_d) for Zn(cy4q)−DNA adducts, derived from a competitive binding model, do not differ markedly from the apparent dissociation constants. The largest difference is observed in K_d for the adducts with RNA hairpins, resulting from the tight binding of EtBr to the bulge and weaker binding to the stem. A comparison of the K_d values shows a 100-fold specificity of Zn(cy4q) for the uracil bulge over the hairpin lacking a bulge.

Binding of the 4-methylquinoline cyclen ligand, without the Zn^{II} metal, to Tgg gave $K_{d(app)}$ of 0.20 mM, 100-fold less tight than the corresponding zinc(II) complex. Binding by the parent complex lacking an aromatic pendent group, Zn(cyclen), gave $K_{d(app)}$ of 2.2 mM to Tgg. These data demonstrate that both the Zn^{II} cation and the pendant quinoline group are necessary for micromolar binding to thymine bulges.

Free Zn^{II} ions at concentrations that would be present from dissociation of the complex do not markedly affect EtBr displacement. For example, Zn(cy4q), Zn(dsc), and Zn(cybp) have less than 1 μM free Zn^{II} ions for solutions containing 100 μM or 10 μM $ZnCl_2$ and a macrocycle in equimolar amounts at pH 7.5 (Table S1 in the Supporting Information). $ZnCl_2$ (5 μM) gives a 1% and 4% displacement of EtBr bound to Tgg or HP3, respectively.

Thermal Denaturation Studies. Optical thermal melting experiments were carried out in the presence of Zn(cy4q) or Zn(cybp), as the most strongly binding complexes, to determine whether the complexes stabilized or destabilized the DNA oligonucleotide structures upon binding. T_m values in the absence and presence of the zinc(II) complex are listed in Tables SI-2−4 in the Supporting Information. It is notable that, even with 3 equiv of the complex, no significant destabilization of the oligonucleotides was observed. Under these conditions, the DNA bulges are fully bound to Zn(cy4q). Figure SI-7 in the Supporting Information shows data for additional studies on the effect of Zn(cy4q) on bulged structures, mostly thymines, with different flanking residues or with increased stem length. Ugg, Tga, and TgaE all show a modest increase in T_m with increasing Zn(cy4q) concentration. Two other bulges, Tgg and TggE, show increases in T_m upon the addition of 1−2 equiv of the zinc(II) complex. This stabilization is consistent with the complex interacting locally with the bulge and possibly its flanking bases to stabilize the structure by stacking interactions. The bulges that contain one or more flanking cytosines, Tcg, TcgE, and Tcc, exhibit a slight destabilization upon the addition of the zinc(II) complex. Zn(cybp) did not change the thermal melting temperature of the fully matched HP4. An increase of 4 °C in T_m was observed in T_m of Tgg upon the addition of 3 equiv of the complex. The other two complexes, Zn(dsc) and Zn(cy2q), did not bind sufficiently strongly to the oligonucleotides to make it feasible to study the effect of bound zinc(II) complex on the optical thermal melting of the DNA.

NMR Studies. The Tgg and TggX hairpins, which both contain a thymine bulge in the stem but have different length stems, were studied using ^{1}H NMR spectroscopy. For simplification and a direct comparison between Tgg and TggX, the numbering scheme for TggX is d(G1-G2-C3-C4-G5-C6-A7-G8-T9-G10-C11-C12) and Tgg is d(G2-C3-C4-G5-C6-A7-G8-T9-G10-C11). As shown previously, the Tgg hairpin binds Zn(cy4q) to give a well-resolved ^{1}H NMR spectrum consistent with a single species in solution of 1:1 stoichiometry (Figure 3), as confirmed by the absence of any changes in the spectrum after the addition of 1.25−2 equiv of the zinc(II)

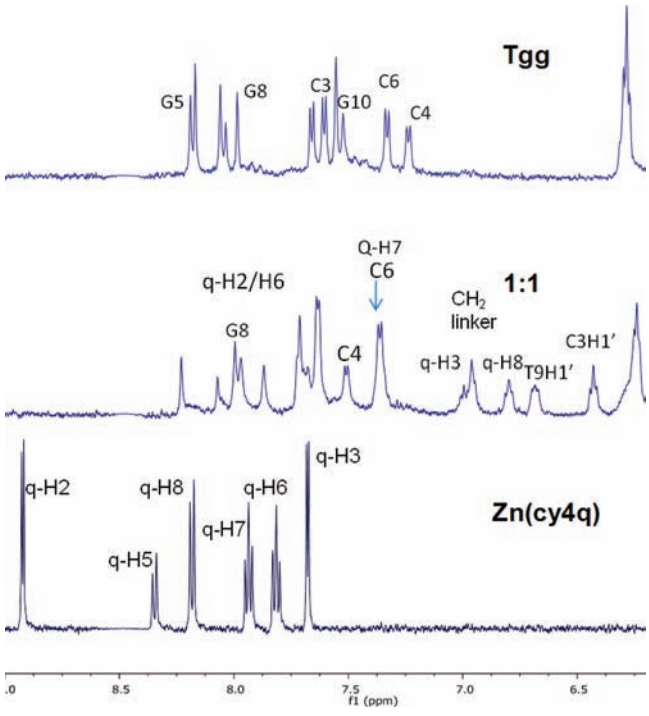

Figure 3. ^{1}H NMR resonances of Tgg, Zn(cy4q), and their 1:1 adduct at 25 °C, 0.10 M NaCl, 0.020 M HEPES, and pH 7.5.

dx.doi.org/10.1021/ic3004245 | Inorg. Chem. 2012, 51, 5444−5457

complex (data not shown).[18] However, the ^{1}H NMR spectrum of the Tgg oligonucleotide at 2 mM in the absence of the zinc(II) complex shows evidence for multiple conformations (Figure SI-8 in the Supporting Information). Thus, the solution structure of a related hairpin loop with a thymine bulge, TggX, was solved for comparison with the ^{1}H NMR data for Tgg-bound Zn(cy4q).

The proton chemical shift of the thymine methyl group of the Tgg hairpin differs slightly from that of thymine in Watson−Crick base pairs and is similar to previously reported bulges with an extrahelical thymine.[67] As previously reported, binding of Zn(cy4q) to the Tgg hairpin leads to a decrease in the intensity of the thymine methyl resonance at 1.7 ppm and the appearance of a new downfield resonance at 2.1 ppm. This is consistent with interaction of the aromatic quinoline moiety of Zn(cy4q) with the bulged thymine in the hairpin stem. In addition to the shifted methyl resonances, five well-resolved proton resonances in the 6.3−7.0 ppm region grow in upon the addition of 1 equiv of Zn(cy4q) to Tgg. These protons are assigned[18] as the C4H1′, T9H4′, the quinoline (q) q-H8 and q-H3 protons, and q-CH_2 protons of the pendent group (Figure 3).

The ^{1}H NMR spectrum of the 2 mM Tgg hairpin sample without Zn(cy4q) indicates that there is more than one conformation in solution. This can be seen clearly in the imino proton region of the spectrum (Figure 4), where the total

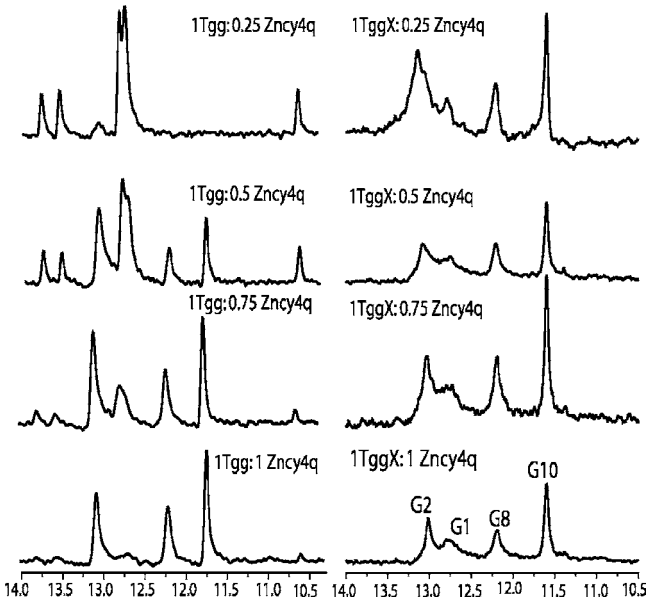

Figure 4. Imino ^{1}H NMR spectra at 5 °C, 2.00 mM HEPES, 0.10 M NaCl, and pH 7.5 for Tgg (left) and TggX (right) titrated with Zn(cy4q).

number of imino proton resonances exceeds the five expected for the Tgg hairpin. Upon binding of the Zn(cy4q) complex, the imino proton spectrum of 2 mM Tgg:Zn(cy4q) exhibits characteristics similar to those of the 0.6 mM Tgg:Zn(cy4q) complex, indicating that binding of Zn(cy4q) favors one conformation in solution. Similarly, the ^{1}H NMR spectrum of Tgg:Zn(cy4q) (0.6 and 2.0 mM) gives the same five well-resolved protons in the 6.3−7.0 ppm region, consistent with the same single conformation in solution at both concentrations of DNA (Figure SI-8 in the Supporting Information). For NMR structural studies of the unbound DNA bulge, TggX was studied because it contains an additional GC base pair to stabilize the stem and favor the hairpin conformation in solution at higher concentrations. In support of this, the 1D imino proton spectrum of TggX contains the correct number of imino resonances, indicating that only one predominant conformation is present in solution (Figure 4). The ^{1}H NMR spectra of Zn(cy4q) bound to either Tgg or TggX show that the q-CH_2, q-H3, q-H8, and T9H1′ protons all shift into the 6.3−7.0 ppm region (Figure SI-9 in the Supporting Information), indicating that Tgg and TggX bind to Zn(cy4q) similarly and that a direct comparison of the these NMR spectra can be made. Analysis of the 2D NOESY spectra of the nonexchangeable protons for Tgg and TggX showed similar crosspeak patterns and chemical shifts (Figures 5 and SI-10 and

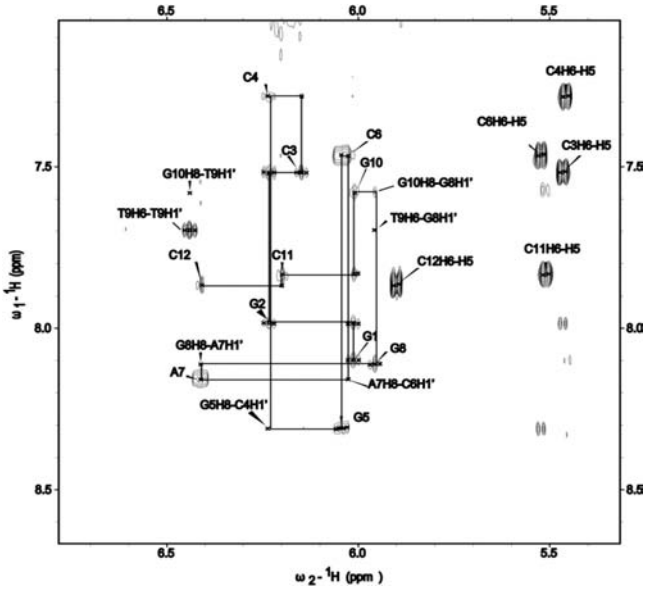

Figure 5. Expanded region of the 500 MHz NOESY spectrum (400 ms, D_2O, 25 °C, 2 mM HEPES, pD 7.9, and 0.1 M NaCl) of TggX showing H6/H8−H1′ sequential connectivity and the H6−H5 cross peaks.

-11 in the Supporting Information). Given that the NMR spectra of Zn(cy4q) bound to the TggX hairpin exhibited line broadening that affected assignments and provided limited information on the structure of the complex, the better-resolved NMR spectra recorded for the bound Tgg:Zn(cy4q) were used to characterize the adduct.

2D NMR Spectral Analysis of TggX. Analysis of the base to H1′ region of the 2D NOESY spectrum provided sequential assignments for TggX (Figure 5). A table of proton chemical shift assignments can be found in Table SI-5 in the Supporting Information. The following NOE cross peaks were weaker than expected or were not observed: G5H8·C4H1′, A7H8·C6H1′, G8H8·A7H1′, T9H6·G8H1′, and G10H8·T9H1′. Despite the lack of NOE connectivity in the base to H1′ region, the base proton assignments were obtained by crosspeak assignments in the H3′ (Figure SI-10 in the Supporting Information) and H2′/H2″ (Figure SI-11 in the Supporting Information) regions. Weak or absent cross peaks between the stem and loop nucleobases (in their H6/H8 connectivity) are good indicators of loop formation.[68] In the base H2′/H2″ region, the missing G5H8·C4H1′ cross peak, not seen in the base−H1′ connectivity, was confirmed by the inter-residue cross peak

dx.doi.org/10.1021/ic3004245 | Inorg. Chem. 2012, 51, 5444−5457

between G5H8 and C4H2″. In DNA containing a GA mismatch, H2′ commonly resonates upfield of H2″. In the TggX hairpin, the G5H2″ resonance is upfield of G5H2′. This ~0.5 upfield shift can be explained by C4 being just below the ring of the G5 base, similar to what Hirao and co-workers observed and modeled.[69] There was also a very strong C6H6 to G5H1′ cross peak and C6−G5 inter-residue connectivity in the H2′/H2″ region, showing a strong stacking interaction of the C6 loop base on G5. Upfield-shifted resonances of the C6 deoxyribose protons including H4′, H5′, and H5″ at 1.3, 3.3, and 3.5 ppm, respectively, further support the formation of the hairpin loop/turn. These protons typically resonate in the 4−4.5 ppm range. The C6H4′ assignment was verified via C6H5′/H5″ to C6H4′ cross peaks in the TOCSY, DQF-COSY, and NOESY data. This unusual 2.7 ppm upfield shift for the H4′ proton and the 0.5 ppm upfield shift of the H5′/H5″ sugar protons has been used as an indication of the deoxyribose moiety of C6 being located directly over the strong ring current of either G5 or A7 nucleobases and is characteristic of loop formation.[69,70]

The NOE between G8H1′ and G10H8 places G8 and G10 stacked on one another, which places the T9 base and sugar rotated out of the helix to accommodate the stacking of G8 and G10 (Figure 5). There are no T9H6 to G8H1′ and G10H8 to T9H1′ sequential cross peaks, indicating that the T9 nucleotide is extrahelical. The weak or absent NOEs to T9H6 and T9Me are consistent with T9 being external to the helix. Table SI-5 in the Supporting Information contains the chemical shift values for the protons in the TggX hairpin. Analysis of the H1′−H2′/H2″ and H3′−H2′/H2″ *J*-coupling patterns in the DQF-COSY spectrum shows that the majority of the sugar geometries are C2′-*endo*. Because of overlap between H1′−H2″ and H1′−H2″ DQF-COSY cross peaks, the G5 sugar geometry could not be determined. On the basis of the crosspeak pattern observed in the 2D NOESY spectrum, G5H1′ exhibits a doublet-of-doublets pattern that is different from that observed for other base-to-H1′ proton cross peaks (Figure 5).

Structure of the TggX Hairpin with a Thymine Bulge. The structural calculations for the TggX hairpin converged to one conformation with a 1.5 Å root-mean-square deviation for the top 20 structures with no distance violations. In Figure 6 (left) is shown the superimposition of the top 20 structures, and Figure 6 (right) shows the structure that best fits the NMR data based on the *f* value calculated by CYANA. The bulged T9 in all of these structures is located in the major groove, with its methyl group pointing outward. The T9 ring lies in the same plane as the C3:G10 base pair, with the O2 carbonyl oxygen pointing into the major groove. This oxygen is in close proximity to the N7 and O4 of G10 and the N4 amine of C3. The C4:G8 and C3:G10 base pairs are partially stacked, with part of the aromatic ring of G8 positioned into the major groove and unstacked. Alignment of the T9 in the major groove appears to form a pocket in which the Zn^{II} center can bind N3 of the thymine and the quinoline can stack on the thymine and possibly interact with G8 and G10 and their base-paired partners C4 and C3.

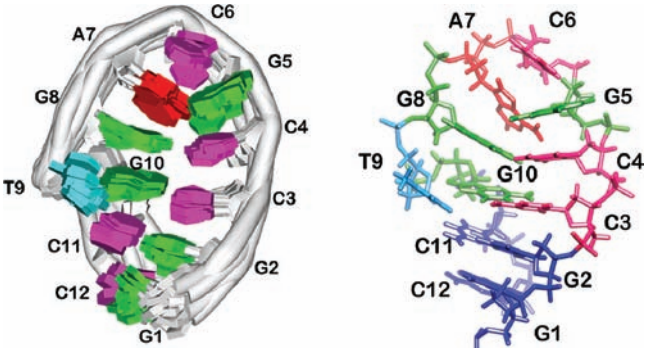

Figure 6. Left: Superposition of 20 TggX structures calculated using CYANA with nucleotides labeled. Right: Structure that best fits the NMR data, with G1, G2, C11, and C12 colored dark blue, T9 light blue, G5, G8, and G10 green, C6 lavender, and A7 red.

NMR Characterization of Zn(cy4q) Bound to Tgg and TggX. NMR data were collected, and the Zn(cy4q) and Tgg proton resonances were assigned. Base and sugar proton assignments are provided in Table SI-6 in the Supporting Information. The base-to-H1′ proton region exhibited few internucleotide NOESY cross peaks. Assignments were made through a comparison to the TggX hairpin NMR data and detailed analysis of the 200 and 400 ms NOESY and DQF-COSY spectra. The cross peaks in the base-to-H2′/H2″ region were sufficient to make internucleotide connectivities and sequential assignments for all but the A7 nucleotide. Upon formation of the Tgg:Zn(cy4q) adduct, the T-H6 and T-Me shift downfield. The upfield shifts of some of the quinoline protons are consistent with them being located within the shielding region of the thymine ring (3−8 Å above and ≤4 Å horizontal to the ring center of the thymine plane). The stacking of the quinoline on the thymine may be slightly skewed, placing the H2, H3, H7, and H8 protons above the thymine ring plane, where they would be upfield-shifted and H5 and H6 in the region where shielding or deshielding effects are minimal so that little or no change in the chemical shift will be observed. There are large changes in the chemical shift observed for the C3, C4, G8, and G10 nucleotides, which comprise the flanking base pairs of the T bulge (Figure 7). The

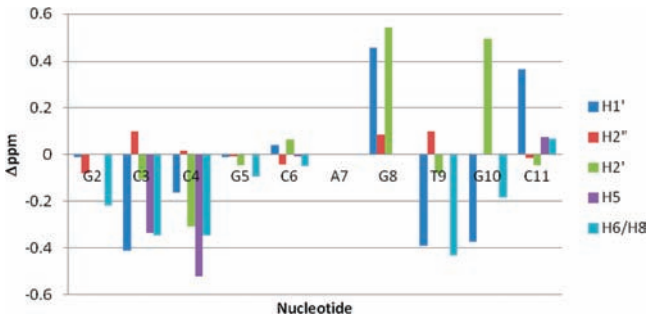

Figure 7. Change in the chemical shift of the Tgg nucleotide protons upon Zn(cy4q) binding. Positive values indicate a downfield shift, and negative values indicate an upfield shift.

C3 and C4 protons exhibit mostly upfield shifts, whereas the assigned G8 protons exhibit downfield chemical shifts. G10H1′ and H8 are upfield shifted and G10H2′ is downfield shifted. These shifts suggest a significant change in the stacking of the C4:G8 and C3:G10 base pairs and the location of the T9 nucleotide.

In Figure 8, 2D NOESY data collected in water shows base-pair imino-to-imino and imino-to-amino NOE connectivities, establishing that the C3:G10 and C4:G8 base pairs are stacked. The G8-to-G10 imino-to-imino NOE is not observed, but the G10 imino to G8 amino NOE is present (Figure 8, peak e),

dx.doi.org/10.1021/ic3004245 | *Inorg. Chem.* 2012, 51, 5444−5457

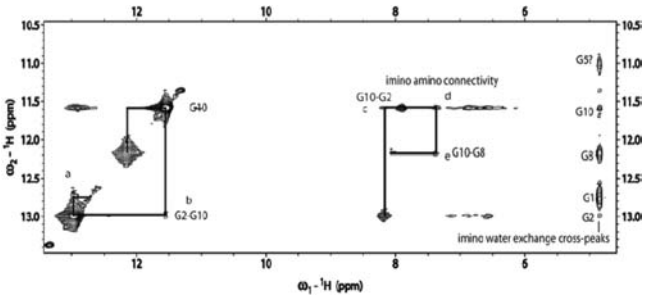

Figure 8. 2D imino–imino and imino–amino connectivity for Tggx with equimolar Zn(cy4q), 1–1 spin–echo NOESY (rna_11NOESY pulse sequence, mixing time = 100 ms, T = 5 °C, I = 0.1 M NaCl, 2.0 mM HEPES, and pH 7.5): (a) NOESY cross peak between G1 and G2 imino protons; (b) NOE between the G2 and G10 imino protons; (c) NOE between the G2 amino and G10 imino; (d) G10 imino to G8 amino proton. Imino exchange cross peaks with water are present.

indicating that these base pairs are partially stacked with G8 base-shifted into the major groove toward T9.

The presence of a single defined set of imino protons after Zn(cy4q) has been added suggests that Zn(cy4q) favors one conformation in solution at 5 °C. The nonexchangeable proton spectra at 20 °C show chemical exchange for the G8 and A7 nucleotides, indicating a more dynamic structure at this temperature. Previous structural studies on thymine bulges show two distinct conformations: one with an internally stacked thymine and the other with an externally oriented thymine.[65] The thymine in the unbound TggX in this study is predominantly external, and Tgg:Zn(cy4q) also favors an extrahelical (looped-out) thymine conformation.

Chemical shift data analysis for the quinoline and Tgg sequence shows that Zn(cy4q) interacts directly with the T bulge. The following NOE interactions define the location and orientation of Zn(cy4q). The quinoline (q) q-H8 and q-H3 protons in Zn(cy4q) exhibit weak NOEs to G8H2″ (Figure 9). The T9H4′, H5′, and H5′ protons exhibit NOEs to only the q-H8 proton, and q-H3 has an NOE to the T9 methyl. These NOEs indicate that the quinoline ring is stacked on T9 and oriented toward the major groove on the 5′ side of T9.

Structure of the Tgg:Zn(cy4q) Adduct. The superposition of the 20 Tgg structures generated using CYANA and the model of the Zn(cy4q):Tgg complex are shown in Figure 10. The limited NOE restraints obtained from the Zn-

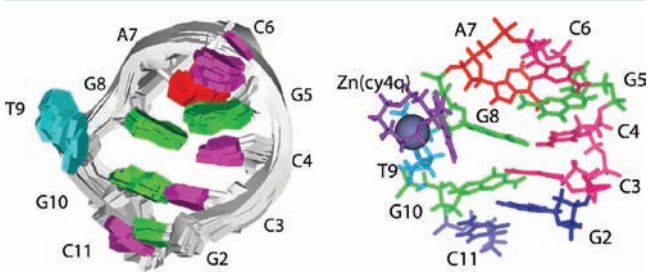

Figure 10. (Left) Superposition of 20 Tgg structures calculated from the Tgg:Zn(cy4q) NOESY data. (Right) One of the structures with the Zn(cy4q) docked. Zn^{II} is in CPK, and cy4q is purple.

(cy4q):Tgg NMR data resulted in the T9 nucleotide being less defined than that in the TggX structure. Therefore, the Tgg structures are considered plausible structures, and only general structural features that are supported by NMR data will be discussed. In the Tgg structures, T9 is rotated out of the major groove further than that in the TggX structures, with its methyl group oriented toward the G8 nucleotide. The outward position of T9 appears to widen the groove to accommodate binding of Zn(cy4q). The Tgg structures have the flanking GC base pairs stacking with each other. In the Zn(cy4q):Tgg model structure, the cyclen ring is located near the hydrogen-bonding surface of T9 and does not interact with the major groove. This is consistent with the lack of NOEs between cyclen CH_2 and DNA protons in the NOESY spectra. The quinoline ring is partially stacked on T9 and fits against the major groove wall near the G8 base and sugar. The nitrogen in the quinoline is oriented toward the major groove near the G8 sugar. In the docked structure, the q-H8 NOEs to T9 and G8 protons are satisfied. In the structure, q-H3 is positioned above the T9 ring close enough to exhibit an NOE to the T9-Me. However, the q-H3 to G8H2″ distance is greater than 5 Å and appears not to fit the NMR data. In order to satisfy the NOEs between the q-H3 and G8H2″ and between the q-H3 and T9-Me, the G8 nucleotide would have to be shifted more into the major groove, with the G8 base positioned above the quinoline ring.

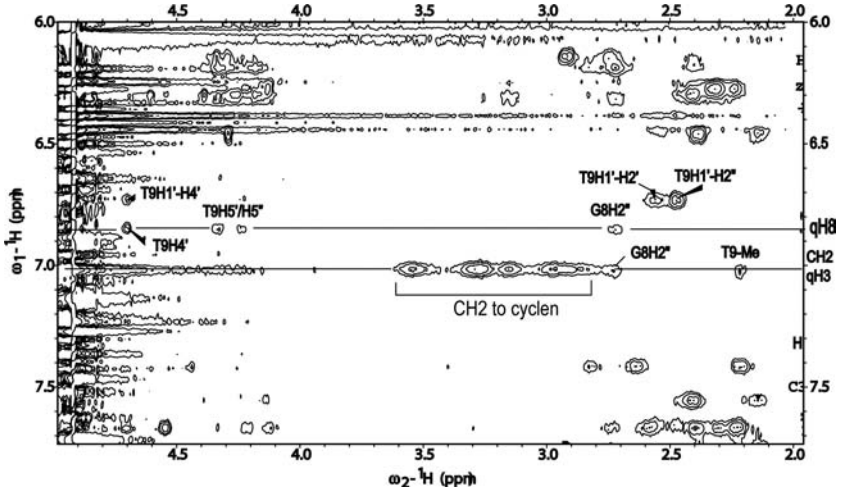

Figure 9. Region of the 2D NOESY spectrum collected at 20 °C in HEPES buffer, pH 7.5, and 010 M NaCl. NOEs between the q-H3, qH8, and T9 and G8 base and sugar protons are shown for the Tgg hairpin with bound Zn(cy4q).

dx.doi.org/10.1021/ic3004245 | Inorg. Chem. 2012, 51, 5444–5457

The chemical shift changes upon binding of Zn(cy4q) are consistent with the orientation and position of the quinoline. T9H1′ lies below the plane of the quinoline ring, where it would be expected to exhibit an upfield shift. G8H1′, H2′, and H2″ lie close to the plane of the quinoline and would be downfield-shifted. G8H8 is located above and toward the edge of the quinoline, where it could exhibit either an upfield or a downfield shift. A change in stacking of the G8 and G10 nucleotide protons would result in changes in their chemical shifts. Because of differences in base stacking in the calculated structures, a rational description of the changes in the proton chemical shifts in the C3, G10, and C4 nucleotides cannot be made.

DISCUSSION

The bifunctional nature of the Zn^{II}(cyclen) derivatives with aromatic pendant groups is an advantage in their development as recognition agents for T bulges in DNA or U bulges in RNA. The Zn^{II} center is selective for binding to unpaired T or U, while the aromatic group can be varied to optimize interactions with the T/U and with the flanking bases in the helix. Our work here shows that both components must work together to optimize binding to DNA sequences containing T bulges. The ∼200-fold selectivity of the Zn(cy4q) complex toward a T bulge over a fully complementary stem and the 50−100-fold stronger binding of a T bulge compared to a C bulge are impressive selectivity for recognition of a pyrimidine bulge. To date, the selectivity obtained here with a coordination complex has been a challenge to attain with organic heterocyclic compounds that recognize the bulged nucleobase through hydrogen-bonding interactions.[11]

The strength of the interaction of the zinc(II) macrocyclic complexes with the thymine N3 anion is related to their water ligand pK_a values. As shown previously, there is a linear correlation of the zinc(II) complex hydroxide binding constant (related to the zinc(II) water ligand pK_a) to the thymine N3 anion binding constant for simple macrocycles with no pendent group.[24] On the basis of this correlation, Zn(dsc) should display slightly stronger thymine binding constants than the other two complexes that have open coordination sites. However, unlike the simple macrocyclic complexes we studied previously, the strength of thymine binding to zinc(II) complexes here will also depend on stacking contributions from the aromatic pendent groups. To gauge the strength of these interactions to thymine in an unstructured context, CCTCC was studied. These studies showed that the binding constant of CCTCC for Zn(cy4q) is 2-fold tighter compared to that of Zn(dsc). This is unexpected given the greater Lewis acidic character of the Zn(dsc) complex and suggests that there is a more favorable stacking interaction of the thymine with the planar quinoline pendent group even in a relatively unstructured DNA. Notably, in the more rigid structural context of a bulge, the thymine is bound 100-fold more strongly to Zn(cy4q) than to Zn(dsc). As shown in the NMR structure, the Zn(cy4q) complex binds to thymine, with the quinoline stacked on the thymine and also interacting with G8 in the major groove.

In contrast, the dansyl group binds less tightly to the bulged thymine than to the more flexible thymine in the single-stranded oligonucleotide. Both the nonplanar nature of the aromatic ring due to the dimethylamino substitutent and the more rigid nature of the sulfone linker may be important factors in determining the thymine structural context for binding of Zn(dsc). Thus, the structural properties of the dansyl group do not favor binding to thymine in bulges, most likely because of the tighter restrictions for the aromatic group stacking on the thymine and the additional interactions of the bulged thymine with the duplex, as described further below. It is noteworthy that Zn(dsc) has been shown to bind to thymine abasic sites; thus, the structural context of the thymine appears to be important for binding of this complex to DNA.[30,53]

The Zn(cy4q) complex shows consistently strong binding to all T bulges with nearly identical binding constants to thymine bulges with flanking purine bases. This suggests that there are properties of the bulged structure that enable the formation of a strong adduct with the zinc(II) complex that are lacking in single-stranded oligonucleotides such as CCTCC. One possibility is that the Zn(cy4q) complex strengthens its interactions with the thymine bulge through additional stabilizing interactions of the complex with groups in the major groove such as possible stacking on G8. Alternatively, additional stabilization may result from interactions in the helix itself induced by Zn(cy4q) binding such as increased stacking of the flanking purine bases. For example, our NMR structural studies confirm that the neighboring guanine bases stack on each other. Also consistent with this alternative, the Zn(cy4q) complex moderately stabilized the T bulges containing two purines as flanking bases upon the addition of up to 3 equiv of complex (2−10 °C) and slightly destabilized a few hairpins containing one or more pyrimidines (−2 to +5 °C).

Binding of Zn(cy4q) to the RNA bulge, Ugg, is tighter than that to the hairpin with no bulge, although the selectivity (2-fold in K_{app} and 100-fold in K_d) is less dramatic than that of the DNA thymine bulges. Binding of Zn(cy2q) or Zn(cybp) to the RNA with bulged uracil was 30-fold weaker than that to Zn(cy4q), again suggesting the importance of a planar aromatic pendent group. Notably, Zn(cy4q) more markedly stabilized the Ugg bulge of RNA than any of the DNA thymine bulges with an increase in T_m of 13 °C.

The NMR structure of the bulged hairpins in the presence and absence of the Zn(cy4q) complex suggests a rationale for the selectivity of binding to bulged thymines. In the absence of the zinc(II) complex, the thymine bulge is extrahelical and positioned in the major groove in the same plane as the G10 base. The external position of the thymine and orientation of G8 and G10 allow for binding of the zinc(II) complex. The NMR structure of the Zn(cy4q) complex with Tgg has the quinoline ring stacked on the T9 base and interacting with the G8 nucleotide. Although the averaged structure does not have G8 and quinoline stacked, there is NOE evidence that suggests that G8 may partially stack some of the time. In the structure reported here, the Zn^{II}(cyclen) moiety attached at the C4 position of the quinoline allows for optimal stacking of the quinoline pendent group on T9. The positioning of the quinoline in the major groove may contribute to the micromolar binding affinity of Zn(cy4q) to thymine bulges. If Zn(dsc) and Zn(cybp) were bound in a similar position, their pendent groups would have less favorable stacking with the thymine and more unfavorable steric interactions with the T9 and G8 sugars. These unfavorable interactions may contribute to their decreased binding affinity.

CONCLUSIONS

We show here that a zinc(II) complex of a tetraazamacrocycle with pendent aromatic group binds with micromolar affinity to thymine bulges in duplexes or in the stems of hairpins with

dx.doi.org/10.1021/ic3004245 | Inorg. Chem. 2012, 51, 5444−5457

good selectivity over fully complementary DNA or bulges containing A, G, or C nucleotides. The aromatic pendent group must be planar and have a flexible linker to allow stacking of the pendent group on the thymine. Here we show that these interactions are strengthened in the context of a thymine as part of a bulged DNA structure. Structural models generated by NMR spectroscopy support further interactions of the Zn^{II}-bound thymine with the duplex and a rearrangement of the bases within the duplex to optimize stacking that may contribute favorably to the stability of the Zn(cy4q) complex with the bulged thymine.

■ ASSOCIATED CONTENT

Supporting Information

Materials/methods, synthesis, NMR spectra, and potentiometric titrations. This material is available free of charge via the Internet at http://pubs.acs.org.

■ AUTHOR INFORMATION

Corresponding Author

*E-mail: matthew.fountain@fredonia.edu (M.A.F.), jmorrow@buffalo.edu (J.R.M.). Tel: 716-673-3287 (M.A.F.), 716-645-4187 (J.R.M.). Fax: 716-645-6963 (J.R.M.).

Notes

The authors declare no competing financial interest.

■ ACKNOWLEDGMENTS

We gratefully acknowledge the National Science Foundation (NSF; Grant CHE-0911375) for support of this work. M.A.F. thanks the NSF for a research opportunity award supplement.

■ REFERENCES

(1) Neidle, S. *FEBS J.* **2010**, *277*, 1118−1125.
(2) Balasubramanian, S.; Neidle, S. *Curr. Opin. Chem. Biol.* **2009**, *13*, 345−353.
(3) Mirkin, S. M. *Nature* **2007**, *447*, 932−940.
(4) Mirkin, S. M. *Curr. Opin. Struct. Biol.* **2006**, *16*, 351−358.
(5) Tang, W.; Dominska, M.; Greenwell, P. W.; Harvanek, Z.; Lobachev, K. S.; Kim, H.-M.; Narayanan, V.; Mirkin, S. M.; Petes, T. D. *PLoS Genet.* **2011**, *7*, e1001270.
(6) Baase, W. A.; Jose, D.; Ponedel, B. C.; von Hippel, P. H.; Johnson, N. P. *Nucleic Acids Res.* **2009**, *37*, 1682−1689.
(7) Loeb, L. A.; Loeb, K. R.; Anderson, J. P. *Proc. Natl. Acad. Sci. U.S.A.* **2003**, *100*, 776−781.
(8) Nishizawa, S.; Sankaran, N. B.; Seino, T.; Cui, Y. Y.; Dai, Q.; Xu, C. Y.; Yoshimoto, K.; Teramae, N. *Anal. Chim. Acta* **2006**, *556*, 133−139.
(9) Rajendar, B.; Sato, Y.; Nishizawa, S.; Teramae, N. *Bioorg. Med. Chem. Lett.* **2007**, *17*, 3682−3685.
(10) Suda, H.; Kobori, A.; Zhang, J.; Hayashi, G.; Nakatani, K. *Bioorg. Med. Chem.* **2005**, *13*, 4507−4512.
(11) Ong, H. C.; Arambula, J. F.; Rao Ramisetty, S.; Baranger, A. M.; Zimmerman, S. C. *Chem. Commun.* **2009**, 668−670.
(12) Nakatani, K.; Okamoto, A.; Saito, I. I. *Angew. Chem., Int. Ed.* **1999**, *38*, 3378−3381.
(13) Kobori, A.; Murase, T.; Suda, H.; Saito, I.; Nakatani, K. *Bioorg. Med. Chem. Lett.* **2004**, *14*, 3431−3433.
(14) Zeglis, B. M.; Boland, J. A.; Barton, J. K. *J. Am. Chem. Soc.* **2008**, *130*, 7530−7532.
(15) Zeglis, B. M.; Boland, J. A.; Barton, J. K. *Biochemistry* **2009**, *48*, 839−849.
(16) Cai, J.; Muller, J. G.; Burrows, C. J. *Supramol. Chem.* **2002**, *14*, 121−126.
(17) Spillane, C. B.; Smith, J. A.; Buck, D. P.; Collins, J. G.; Keene, F. R. *Dalton Trans.* **2007**, 5290−6.
(18) del Mundo, I. M. A.; Fountain, M. A.; Morrow, J. R. *Chem. Commun.* **2011**, *47*, 8566−8568.
(19) Aoki, S.; Kimura, E. *Chem. Rev.* **2004**, *104*, 769−87.
(20) Kimura, E.; Kitamura, H.; Ohtani, K.; Koike, T. *J. Am. Chem. Soc.* **2000**, *122*, 4668−4677.
(21) Shionoya, M.; Ikeda, T.; Kimura, E.; Shiro, M. *J. Am. Chem. Soc.* **1994**, *116*, 3848−3859.
(22) Schmidt, F.; Stadlbauer, S.; Konig, B. *Dalton Trans.* **2010**, *39*, 7250−7261.
(23) Subat, M.; Borovik, A. S.; Konig, B. *J. Am. Chem. Soc.* **2003**, *126*, 3185−3190.
(24) Rossiter, C. S.; Mathews, R. A.; Morrow, J. R. *Inorg. Chem.* **2005**, *44*, 9397−9404.
(25) Shionoya, M.; Suglyama, M.; Kimura, E. *J. Chem. Soc., Chem. Commun.* **1994**, 1747−1748.
(26) Kimura, E.; Ikeda, T.; Aoki, S.; Shionoya, M. *J. Biol. Inorg. Chem.* **1998**, *3*, 259−267.
(27) Kikuta, E.; Katsube, N.; Kimura, E. *J. Biol. Inorg. Chem.* **1999**, *4*, 431−440.
(28) Kikuta, E.; Aoki, S.; Kimura, E. *J. Am. Chem. Soc.* **2001**, *123*, 7911−7912.
(29) Le Baccon, M.; Chuburu, F.; Toupet, L.; Handel, H.; Soibinet, M.; Dechamps-Olivier, I.; Barbiere, J. P.; Aplincourt, M. *New J. Chem.* **2001**, *25*, 1168−1174.
(30) O'Neil, L. L.; Wiest, O. *J. Am. Chem. Soc.* **2005**, *127*, 16800−16801.
(31) Gans, P.; Sabatini, A.; Vacca, A. *Talanta* **1996**, *43*, 1739−1753.
(32) McDowell, J. A.; Turner, D. H. *Biochemistry* **1996**, *35*, 14077−14089.
(33) Waring, M. J. *J. Mol. Biol.* **1965**, *13*, 269−282.
(34) Suh, D.; Chaires, J. B. *Bioorg. Med. Chem.* **1995**, *3*, 723−728.
(35) Izumrudov, V. A.; Zhiryakova, M. V.; Goulko, A. A. *Langmuir* **2002**, *18*, 10348−10356.
(36) Boger, D. L.; Fink, B. E.; Brunette, S. R.; Tse, W. C.; Hedrick, M. P. *J. Am. Chem. Soc.* **2001**, *123*, 5878−91.
(37) Satz, A. L.; Bruice, T. C. *Bioorg. Med. Chem.* **2000**, *8*, 1871−1880.
(38) White, S. A.; Draper, D. E. *Nucleic Acids Res.* **1987**, *15*, 4049−4064.
(39) Stootman, F. H.; Fisher, D. M.; Rodger, A.; Aldrich-Wright, J. R. *Analyst* **2006**, *131*, 1145−1151.
(40) Piotto, M.; Saudek, V.; Sklenar, V. *J. Biomol. NMR* **1992**, *2*, 661−665.
(41) Sklenar, V.; Bax, A. *J. Magn. Reson.* **1987**, *74*, 469−749.
(42) Bax, A.; Davis, D. G. *J. Magn. Reson.* **1985**, *63*, 207−213.
(43) Davis, D. G.; Bax, A. *J. Am. Chem. Soc.* **1985**, *107*, 2820−2821.
(44) Bax, A. *Methods Enzymol.* **1989**, *176*, 151−168.
(45) Rance, M.; Sorensen, O. W.; Bodenhausen, G.; Wagner, G.; Ernst, R. R.; Wuthrich, K. *Biochem. Biophys. Res. Commun.* **1983**, *117*, 479−485.
(46) Piantini, U.; Sorensen, O. W.; Ernst, R. R. *J. Am. Chem. Soc.* **1982**, *104*, 6800−6801.
(47) Goddard, T. D. K., D. G.; *SPARKY 3 NMR software*; University of California: San Francisco, CA, 2001 (www.cgi.ucsf.edu/home/sparky).
(48) Guntert, P.; Mumenthaler, C.; Wuthrich, K. *J. Mol. Biol.* **1997**, *273*, 283−298.
(49) Guntert, P. *Methods Mol. Biol.* **2004**, *278*, 353−378.
(50) Ohshima, R.; Kitamura, M.; Morita, A.; Shiro, M.; Yamada, Y.; Ikekita, M.; Kimura, E.; Aoki, S. *Inorg. Chem.* **2010**, *49*, 888−899.
(51) Lin, W.-Y.; Van Wart, J. E. *Biochemistry* **1988**, *27*, 5054−5061.
(52) Mathews, R. A.; Rossiter, C. S.; Morrow, J. R.; Richard, J. P. *Dalton Trans.* **2007**, 3804−3811.
(53) O'Neil, L. L.; Wiest, O. *Org. Biomol. Chem.* **2008**, *6*, 485−492.
(54) Kimura, E.; Katsube, N.; Koike, T.; Shiro, M.; Aoki, S. *Supramol. Chem.* **2002**, *14*, 95−102.
(55) LePecq, J. B.; Paoletti, C. *J. Mol. Biol.* **1967**, *27*, 87−106.
(56) Baguley, B. C.; Falkenhaug, E. M. *Nucleic Acids Res.* **1978**, *5*, 161−171.

(57) Krugh, T. R.; Hook, J. W., III; Lin, S.; Chen, F.-M. In *Stereodynamics of Molecular Systems*; Sarma, R. H., Ed.; Permagon Press: London, 1979; pp 423−435.
(58) Chaires, J. B.; Shi, X. In *Sequence-specific DNA binding agents*; Waring, M., Ed.; Royal Society of Chemistry: Cambridge, U.K., 2006.
(59) Krugh, T. R.; Wittlin, F. N.; Cramer, S. P. *Biopolymers* **1975**, *14*, 197−210.
(60) Neidle, S.; Abraham, Z. *Crit. Rev. Biochem. Mol. Biol.* **1984**, *17*, 73−121.
(61) Nelson, J. W.; Tinoco, I., Jr. *Biochemistry* **1985**, *24*, 6416−64121.
(62) White, S. A.; Draper, D. E. *Biochemistry* **1989**, *28*, 1892−1897.
(63) Boger, D. L.; Fink, B. E.; Hedrick, M. P. *J. Am. Chem. Soc.* **2000**, *122*, 6382−6394.
(64) Jenkins, T. C. In *Methods Molecular Biology*; Fox, K. R., Ed.; Humana Press: Totowa, NJ, 1997; Vol. *90*; p 195.
(65) Ikeda, H.; Nakamura, M.; Ise, N.; Toda, F.; Ueno, A. *J. Org. Chem.* **1997**, *62*, 1411−1418.
(66) Janiak, C. *Dalton Trans.* **2000**, 3885−3896.
(67) Kalnik, M. W.; Norman, D. G.; Li, B. F.; Swann, P. F.; Patel, D. J. *J. Biol. Chem.* **1990**, *265*, 636−647.
(68) Colgrave, M. L.; Williams, H. E. L.; Searle, M. S. *Angew. Chem., Int. Ed.* **2002**, *41*, 4754−4756.
(69) Hirao, I.; Kawai, G.; Yoshizawa, S.; Nishimura, Y.; Ishido, Y.; Watanabe, K.; Miura, K. *Nucleic Acids Res.* **1994**, *22*, 576−582.
(70) Zhu, L.; Chou, S. H.; Xu, J.; Reid, B. R. *Nat. Struct. Biol.* **1995**, *2*, 1012−1017.